



# HHS Public Access

Author manuscript

*N Engl J Med.* Author manuscript; available in PMC 2022 August 19.

Published in final edited form as:

*N Engl J Med.* 2021 August 19; 385(8): 761–763. doi:10.1056/NEJMc2101264.

## Lorlatinib in a Child with *ALK*-Fusion–Positive High-Grade Glioma

**Aditi Bagchi, M.D., Ph.D.,**

St. Jude Children's Research Hospital Memphis, TN

**Brent A. Orr, M.D., Ph.D.,**

St. Jude Children's Research Hospital Memphis, TN

**Olivia Campagne, Pharm.D.,**

St. Jude Children's Research Hospital Memphis, TN

**Sandeep Dhanda, Ph.D.,**

St. Jude Children's Research Hospital Memphis, TN

**Sreenath Nair, Ph.D.,**

St. Jude Children's Research Hospital Memphis, TN

**Quynh Tran, Ph.D.,**

St. Jude Children's Research Hospital Memphis, TN

**Anthony M. Christensen, Pharm.D.,**

St. Jude Children's Research Hospital Memphis, TN

**Amar Gajjar, M.D.,**

St. Jude Children's Research Hospital Memphis, TN

**Larissa V. Furtado, M.D.,**

St. Jude Children's Research Hospital Memphis, TN

**Aksana Vasilyeva, Ph.D.,**

St. Jude Children's Research Hospital Memphis, TN

**Frederick Boop, M.D.,**

Le Bonheur Children's Hospital Memphis, TN

**Clinton Stewart, Pharm.D.,**

St. Jude Children's Research Hospital Memphis, TN

**Giles W. Robinson, M.D.**

St. Jude Children's Research Hospital Memphis, TN

---

[giles.robinson@stjude.org](mailto:giles.robinson@stjude.org) .

Disclosure forms provided by the authors are available with the full text of this letter at [NEJM.org](https://www.nejm.org).

## TO THE EDITOR:

Advancements in molecular diagnostics have led to the identification of a new class of pediatric gliomas — infantile hemispheric gliomas — that arise in the cerebral hemispheres and often are histologically confirmed to be malignant (World Health Organization grade III or IV).<sup>1,2</sup> These gliomas harbor receptor tyrosine kinase rearrangements in *ALK*, *ROS1*, *NTRK1/2/3*, and *MET* and are more amenable to therapy, with better survival outcomes, than other pediatric high-grade gliomas.<sup>1,2</sup>

Despite better survival outcomes, management of infantile hemispheric gliomas remains challenging. Given that these gliomas manifest as very large, vascular tumors in the developing brain, the combination of neurosurgery, chemotherapy, and radiation most often results in neurocognitive delays, neuroendocrine deficiencies, and a shortened life span.<sup>2,3</sup>

Here, we report the case of a 3-year-old boy who was brought to the emergency department obtunded after 2 to 3 weeks of vomiting, excessive sleepiness, and exotropia. Magnetic resonance imaging (MRI) of the head revealed a large tumor in the left cerebral hemisphere (Fig. 1A, subpanel a). Two attempts at surgery were halted owing to life-threatening intracranial bleeding, and only a partial resection was achieved. Neoadjuvant chemotherapy was tried. However, after another intracranial bleeding event, further intervention was judged futile. A do-not-resuscitate order was issued, and comfort measures were initiated (Fig. 1A, subpanels b and c). Unexpectedly, despite withdrawal of life support, the patient's breathing and vital signs normalized.

Neuropathological assessment showed a high-grade astrocytic tumor diffusely immunoreactive for *ALK*. Methylation profiling confirmed a tumor of the infantile hemispheric glioma class (Fig. 1C), and RNA sequencing revealed a *SPECC1L-ALK* fusion (Fig. 1D, and Fig. S2 in the Supplementary Appendix, available at [NEJM.org](https://www.nejm.org)).

Considering the patient's clinical status and the finding of *ALK* fusion, lorlatinib was chosen as therapy on the basis of promising data on intracranial response in adults with non-small-cell lung cancer.<sup>4</sup> After informed consent was obtained from the patient's parents, treatment with lorlatinib was initiated by nasogastric tube at a dose of 95 mg per square meter of body-surface area once daily (a dose derived from that administered in a pediatric refractory neuroblastoma cohort<sup>5</sup>).

The patient began to recover, and his neurologic function steadily returned as the tumor shrank. The most notable adverse event was weight gain, which continued despite a 20% reduction in the dose of lorlatinib. After 8 months of treatment, MRI showed that the tumor had been replaced by cystic structures, with only a small residual tumor remaining (Fig. 1A, subpanels d through g, and Fig. 1B). Exploratory surgery was performed to clean out the cavity. Pharmacokinetic studies were performed (with informed consent) before, during, and after surgery. Samples of blood, cerebrospinal fluid, and tumor tissue were analyzed. A gross total resection was achieved, and analyses showed lorlatinib in the tumor at concentrations similar to those found in plasma (Fig. 1E). Comparison of histologic findings before and after treatment with lorlatinib showed a marked decrease in the proliferative

index of the tumor, a finding consistent with a drug-induced response (Fig. 1F). Repeat RNA sequencing detected the *SPECCIL-ALK* fusion, albeit at a low allele frequency.

Therapy was stopped once no tumor was seen on postsurgical MRI (Fig. 1A, subpanel h). However, after 6 months, facial palsy developed in the patient, and new metastatic lesions were identified on cranial nerve VII, within the third ventricle, and on the spine (Fig. 1A, subpanel j, and Fig. S1). Treatment with lorlatinib was resumed at a dose of 95 mg per square meter administered by mouth once daily, and once more the patient had a rapid response. The palsy resolved within a week after treatment resumed, and a follow-up MRI after 1 month showed a near-complete response to treatment in all lesions (Fig. 1A, subpanel k, Fig. 1B, and Fig. S1).

At present, our patient continues to receive lorlatinib therapy and attends preschool without any appreciable neurologic deficits or complications from surgery. Adverse reactions have been limited to weight gain (grade 2 according to the National Cancer Institute Common Terminology Criteria for Adverse Events [CTCAE], version 5) and hypercholesterolemia (CTCAE grade 1). Given the patient's young age and the recent recurrence, we plan to continue therapy, absent any serious side effects, for as long as the disease remains controlled, so that more-damaging chemotherapy or radiation can be avoided or delayed.

ALK inhibitors biochemically developed to penetrate the central nervous system, such as lorlatinib,<sup>4</sup> can affect primary tumors of the central nervous system that harbor target lesions and warrant investigation in the management of *ALK*-fused glioma.

## Supplementary Material

Refer to Web version on PubMed Central for supplementary material.

## Acknowledgments

The content is solely the responsibility of the authors and does not necessarily represent the official views of the funding sources.

Supported by American Lebanese Syrian Associated Charities and a grant (P30CA021765) from the National Cancer Institute Cancer Center.

## References

1. Guerreiro Stucklin AS, Ryall S, Fukuoka K, et al. Alterations in *ALK/ROS1/NTRK/MET* drive a group of infantile hemispheric gliomas. *Nat Commun* 2019; 10: 4343. [PubMed: 31554817]
2. Clarke M, Mackay A, Ismer B, et al. Infant high-grade gliomas comprise multiple subgroups characterized by novel targetable gene fusions and favorable outcomes. *Cancer Discov* 2020; 10:942–63. [PubMed: 32238360]
3. El-Ayadi M, Ansari M, Sturm D, et al. High-grade glioma in very young children: a rare and particular patient population. *Oncotarget* 2017;8: 64564–78. [PubMed: 28969094]
4. Shaw AT, Bauer TM, de Marinis F, et al. First-line lorlatinib or crizotinib in advanced *ALK*-positive lung cancer. *N Engl J Med* 2020; 383:2018–29. [PubMed: 33207094]
5. Goldsmith KC, Kayser K, Groshen SG, et al. Phase I trial of lorlatinib in patients with *ALK*-driven refractory or relapsed neuroblastoma: a New Approaches to Neuroblastoma Consortium study. *J Clin Oncol* 2020; 38(15):Suppl: 10504. abstract.

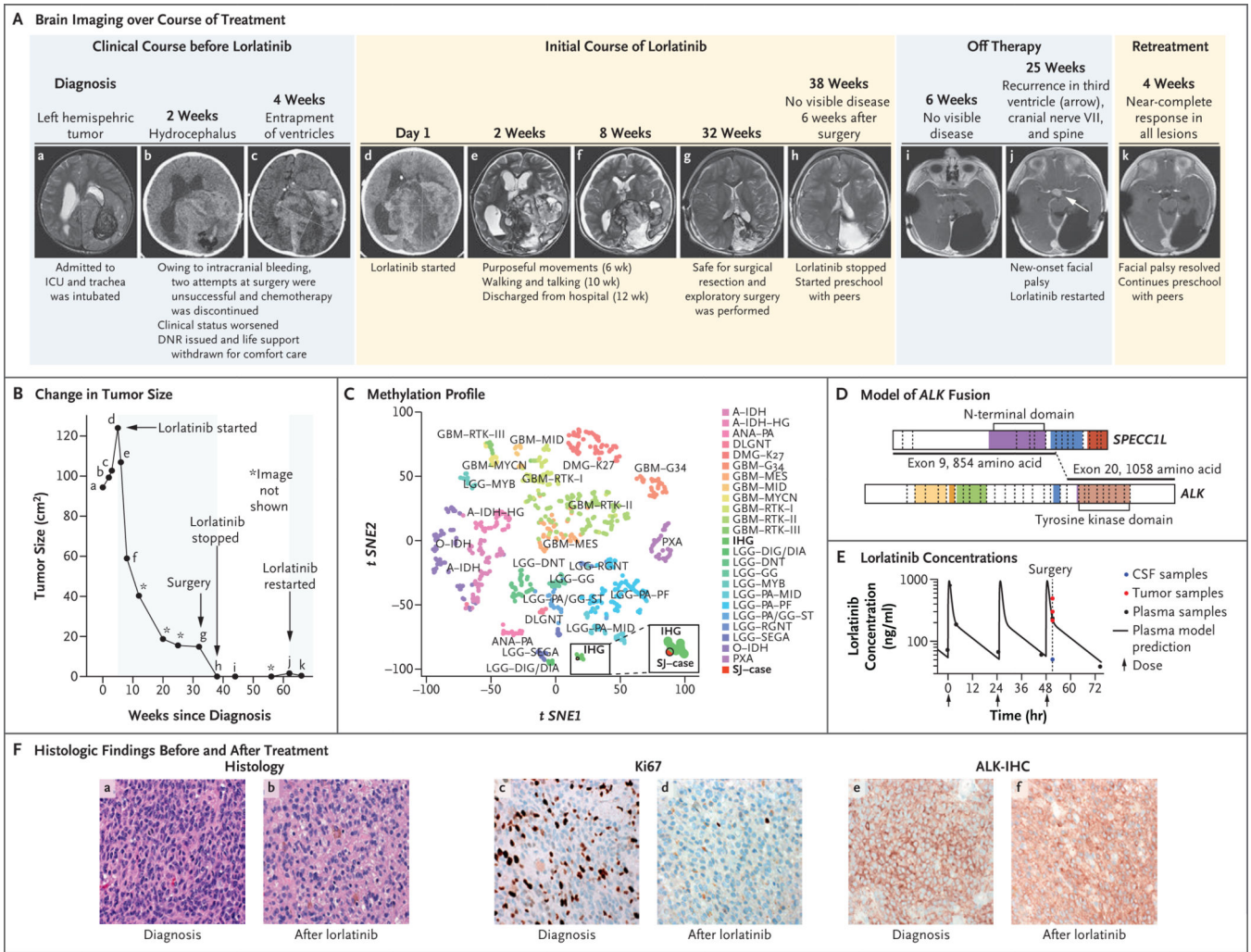


**Figure 1. Response to Lorlatinib Treatment.**

The clinical course of the patient is shown in serial brain imaging taken before (Panel A, subpanels a through c) and during (d through h) initial lorlatinib therapy. Subpanels i and j depict imaging after lorlatinib was discontinued, and subpanel k depicts the near-complete response of the recurrent tumor 4 weeks after retreatment with lorlatinib began. Panel B shows the change in the tumor size (black line) as a function of time and treatment; the black dots (a through k) correspond to the imaging studies shown in Panel A, and shaded areas denote periods of time the patient was receiving treatment with lorlatinib. Tumor size was determined by the product of the measurement of the longest tumor dimension and its perpendicular measurement. Panel C depicts the tumor sample (SJ-case) among infantile hemispheric gliomas (IHG) when projected on a t-statistic-based stochastic neighbor embedding (*t-SNE*) projection of a methylation data set of 1013 gliomas and glioneuronal tumors. Panel D shows a model reconstruction of the in-frame *SPECCIL-ALK* fusion that combined exons 1 through 9 of *SPECCIL* with exons 20 through 29 of *ALK*. The kinase domain of *ALK* (light brown) remained intact. Panel E shows the plasma concentration time of lorlatinib and the lorlatinib concentrations in tumor tissue (red) and cerebrospinal fluid (CSF, blue). The y axis represents measured concentration of lorlatinib.

The x axis represents time in hours; the arrows indicate the times when the patient was administered the medication. Panel F compares the diagnostic sample (a, c, and e) with the sample obtained after treatment with lorlatinib (b, d, and f). The diagnostic sample consisted of a compact, high-grade astrocytoma with mitotic activity (a) and a high proliferative index (c). Strong, diffuse expression of ALK was detected by immunohistochemistry (e). The recurrent tumor showed evidence of therapeutic response, including extensive infiltration by histiocytes (b) and a reduced proliferative index (d). Expression of ALK was retained in the recurrent tumor cells (f). DNR denotes do not resuscitate, and ICU intensive care unit. A key to the abbreviations for the methylation class shown in Panel C is provided in Table S1 of the Supplementary Appendix, available at [NEJM.org](https://www.nejm.org).

Author Manuscript

Author Manuscript

Author Manuscript

Author Manuscript